

# Estimating gravitational radiation from super-emitting compact binary systems

Chad Hanna,<sup>1,\*</sup> Matthew C. Johnson,<sup>2,3,†</sup> and Luis Lehner<sup>3,‡</sup>

<sup>1</sup>*The Pennsylvania State University, University Park, Pennsylvania 16802, USA*

<sup>2</sup>*Department of Physics and Astronomy, York University, Toronto, Ontario M3J 1P3, Canada*

<sup>3</sup>*Perimeter Institute for Theoretical Physics, Waterloo, Ontario N2L 2Y5, Canada*

(Received 10 February 2017; published 26 June 2017)

Binary black hole mergers are among the most violent events in the Universe, leading to extreme warping of spacetime and copious emission of gravitational radiation. Even though black holes are the most compact objects they are not necessarily the most efficient emitters of gravitational radiation in binary systems. The final black hole resulting from a binary black hole merger retains a significant fraction of the premerger orbital energy and angular momentum. A nonvacuum system can in principle shed more of this energy than a black hole merger of equivalent mass. We study these super-emitters through a toy model that accounts for the possibility that the merger creates a compact object that retains a long-lived time-varying quadrupole moment. This toy model may capture the merger of (low mass) neutron stars, but it may also be used to consider more exotic compact binaries. We hope that this toy model can serve as a guide to more rigorous numerical investigations into these systems.

DOI: [10.1103/PhysRevD.95.124042](https://doi.org/10.1103/PhysRevD.95.124042)

## I. INTRODUCTION

The first detections of gravitational waves by the LIGO and Virgo collaborations [1,2] have ushered in the era of gravitational wave astronomy. Both observed events, GW150914 and GW151226, are consistent with the merger of two stellar-mass black holes. Although the collaborations have confirmed that there were no detections of systems containing matter during advanced LIGO's first observing run, they anticipate making detections of systems containing neutron stars in the next few years as advanced LIGO's sensitivity increases [3] and VIRGO joins the detector network.

Binary black holes are regarded as ideal sources of strong gravitational waves, and the recent detections have clearly confirmed this expectation. It is also customary to consider binary black holes giving rise to scenarios capable of radiating most efficiently in gravitational waves. This expectation is supported by the fact that intense gravitational fields and high speeds are probed in the merger of black holes and thus the peak strain can be correspondingly large. Although a large peak strain allows a great deal of information to be gleaned about the final, nonlinear, stages of merger, it does not necessarily yield the most detectable source of gravitational waves nor does it imply binary black holes would emit the most energy for a given mass in quasi-circular encounters.

A gravitational wave detector is sensitive to the total energy impinging on the detector within its frequency

sensitivity, making a merger that emits more energy over longer time scales potentially more detectable than a black hole merger of equivalent mass. In a binary black hole merger, a significant portion of the orbital angular momentum at coalescence is retained in the angular momentum of the resulting Kerr black hole [4]. A merger event of equivalent mass that could shed more of its initial orbital binding energy in a merger could emit a larger total energy in gravitational waves, and therefore be, in principle, more detectable.

One candidate for such a “super-emitting” event is a binary neutron star system which forms a long-lived neutron star as a result of the merger. Such a star spins down as angular momentum is radiated away in gravitational radiation [7–9]. This radiative stage will come to an end when either the massive neutron star that results from the merger stops rotating or its time-dependent quadrupole moment vanishes. Such different types of behavior allowed by neutron stars is also representative, at a qualitative level, to the type of phenomenology that other more exotic objects might provide. Whether a binary neutron star or another more exotic compact binary system can in principle emit more total energy than a black hole binary depends, as we shall discuss below, to leading order on the compaction  $C = GM/R$  of the merging objects with  $M$ ,  $R$  the mass and radius of the object respectively and  $G$  Newton's constant (and the speed of light  $c$  has been set to 1). For neutron stars,  $C \sim 10^{-1}$  and, more generally, exotic compact objects can have a somewhat larger compaction and could emit significantly more total energy than a black hole merger of equivalent mass. Of course, for sufficiently large individual masses in binary neutron star systems, a prompt collapse to a black hole ensues [10] (see e.g. [11]). Since the

\*crh184@psu.edu

†mjohnson@perimeterinstitute.ca

‡llehner@perimeterinstitute.ca

gravitational wave strain is proportional to the chirp mass, low masses have a low chirp mass and thus the detectability horizon is lower. On the other hand, possible massive exotic compact objects—of which there is not certainty on possible mass bounds—could have a farther horizon and the absence of detection from such objects would significantly constrain their existence.

Assessing the amount of energy that can be radiated and the characteristics of gravitational waves produced by generic compact binary mergers provides guidance into the observational opportunities ahead. In this paper, we investigate the gravitational radiation emitted in a simple model binary system composed of spherically symmetric, nonrotating compact objects, and assess the detectability of such events. While we expect this model to be quite far from realistic systems, it can provide a rule of thumb for the qualitative range of signatures that could be expected in principle. In particular, rather than concentrating on the radiative properties of binaries composed of specific exotic objects (e.g. [12,13]) our model accounts for alternatives in a simplistic manner with the goal of extracting the broad qualitative features that general compact systems in quasicircular mergers can yield. For the sake of presentation, and departing slightly from the standard convention, throughout our discussion, we will reserve the term “compact object” to refer to objects which are not black holes—e.g. neutron stars (NS) and exotic compact objects (ECO). Such objects do not have an event horizon but give rise to strong gravitational fields in their vicinity. Additionally we will often employ the term “merger” to denote the full dynamics of the binary; i.e. inspiral, collision, post-merger and final state stages.

## II. A MODEL FOR BINARY SUPER-EMITTERS

Before describing our simple model for nonvacuum binaries, recall the standard binary black hole scenario. The absolute bound on the energy radiated from a binary black hole system comes from black hole thermodynamics. In order for the entropy of the final merged black hole to be nondecreasing, the area of the final black hole must be at least as large as the area of the two initial black holes [14]. Since area scales as  $M^2$ , the final mass,  $M_f$ , obeys  $M_1^2 + M_2^2 \leq M_f^2$  for non-rotating black holes, implying for equal mass binaries that  $\sqrt{2}M \leq M_f \leq 2M$ . This yields a maximum gravitational radiation efficiency of 29% of the binary mass. In order for the final black hole to have no rotation, and for this bound to be satisfied, all of its angular momentum would need to be radiated away during the merger, or somehow extracted via the interactions with additional fields (e.g. via the Penrose, Blandford-Znajek processes [15,16] and related), in which case it would no longer be a pure vacuum binary black hole spacetime. Numerical relativity predictions for nonrotating, equal-mass black holes indicate such cases have a lower

efficiency radiation loss at  $\sim 4\%$  of the binary mass [17] scaling with  $\eta^2$ , where  $\eta = M_1 M_2 / (M_1 + M_2)^2 \leq 0.25$ , for a fixed total mass. The predicted gravitational radiation efficiency has been confirmed observationally with GW150914 which radiated  $\sim 5\%$  of its mass in gravitational waves [1]. We will therefore consider  $\sim 4\text{--}5\%$  to be the threshold beyond which an equal mass compact binary system, with individual objects without intrinsic angular momentum, will be said to radiate more than its binary black hole counterpart.

Our model consists of two nonspinning, spherical compact objects as depicted in Fig. 1. The heavier object has mass  $M_1$ , radius  $R_1$ , and moment of inertia  $\mathcal{I}_1$ ; the lighter object mass  $M_2$ , radius  $R_2$ , and moment of inertia  $\mathcal{I}_2$ . Our toy model includes three phases of evolution: inspiral, post-merger, and final fate. In the inspiral phase, the persistent emission of gravitational radiation causes the compact objects to undergo a slowly decaying nearly circular Keplerian orbit about the center of mass. The center of mass is located a distance  $\Delta_{1,2}$  from each respective mass, and a distance  $\Delta \equiv \Delta_1 + \Delta_2$  from each other. As the objects come into contact, we define the post-merger phase as the time at which the separation between the objects is approximately constant and some fraction of the orbital energy is converted to gravitational radiation. This is in contrast to a binary black hole coalescence, which is characterized by a quick plunge from an approximate inner most stable circular orbit (ISCO). We also allow for the possibility that energy is released in other nongravitational-wave forms e.g. electromagnetic radiation, neutrinos and mass shedding denoted as  $E_{\text{other}}$ . After some time, the merged object achieves its “final fate” which is defined by

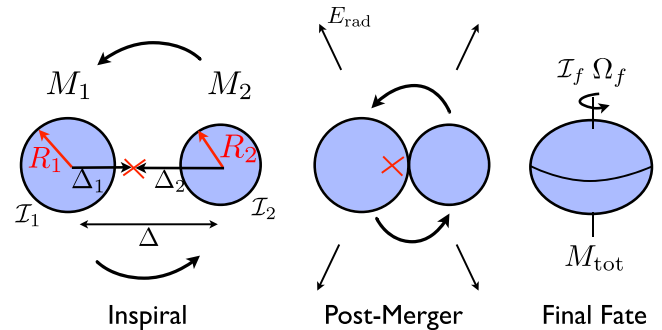


FIG. 1. A toy model for compact object quasicircular merger. During the inspiral phase, two objects of mass  $M_{1,2}$  and radius  $R_{1,2}$  (we assume  $M_1 \geq M_2$ ) undergo a nearly spherical decaying Keplerian orbit about their center of mass (located a distance  $\Delta_{1,2}$  from masses 1 and 2 respectively). Once the objects come into contact, they undergo a merged phase during which orbital energy is converted to gravitational radiation and possibly other forms of radiation (of total energy  $E_{\text{other}}$ ). After some time, the objects merge into an axisymmetric object of constant density with mass  $M_{\text{tot}} \approx M_1 + M_2$  with moment of inertia  $\mathcal{I}_f$  rotating at a constant angular velocity  $\Omega_f$ .

having no residual quadrupole moment (e.g. an axisymmetric or nonrotating object). The mass of the final object is assumed to be approximately conserved,  $M_{\text{tot}} \simeq M_1 + M_2$ , i.e., the stars do not shed significant mass, and any residual rotational energy is locked into the spin of the final object at angular frequency  $\Omega_f$ . Below, it will be useful to write quantities in terms of the compaction of the initial and final objects  $C_i = GM_i/R_i$ ; with  $i = 1, 2, f$  labelling object 1, 2 or the final object respectively.

### A. Energy emitted in gravitational waves

During the inspiral phase, the objects orbit at an instantaneous angular frequency  $\Omega_{\text{insp}}$  about the center of mass, which to leading order, is given by the Keplerian expression  $\Omega_{\text{insp}} = \sqrt{GM_{\text{tot}}/\Delta^3}$ . The center of mass is located a distance  $\Delta_{1,2} = M_{2,1}\Delta/M_{\text{tot}}$  from mass 1 and 2 respectively. Setting the energy to zero for infinitely separated objects, the total change in energy during the inspiral phase due to gravitational wave emission can be estimated as the total energy at the moment when the objects come into contact,

$$\Delta E_{\text{insp}} = \left( -\frac{GM_1M_2}{\Delta} + \frac{1}{2}\mathcal{I}\Omega_{\text{insp}}^2 \right)_{\Delta=R_1+R_2}. \quad (1)$$

The moment of inertia  $\mathcal{I}$  is given by,

$$\mathcal{I} = \tilde{\mathcal{I}}_1 M_1 R_1^2 + \tilde{\mathcal{I}}_2 M_2 R_2^2 + \mu \Delta^2, \quad (2)$$

where  $\mu = M_1 M_2 / M_{\text{tot}}$  is the reduced mass and we have chosen to parametrize the moment of inertia of the initial state objects by dimensionless constants  $\tilde{\mathcal{I}}_{1,2}$ . For constant density spheres,  $\tilde{\mathcal{I}}_{1,2} = 2/5$ , while a more realistic distribution of mass would yield somewhat smaller values of  $\tilde{\mathcal{I}}_{1,2}$  (e.g. [18]).

Once the objects come into contact, they no longer execute a Keplerian orbit and the understanding of the binary's dynamics requires a more delicate analysis including further physics. For instance, in the case of binary neutron stars, nonlinear, general relativistic magnetohydrodynamics accounting for relevant microphysics in the system (see e.g. [8] and references therein) should be considered. With the purpose of deriving an upper bound for generic objects, here we envision a highly idealized post-merger phase, where at the initial contact stage, the objects do not deform and simply fuse into a “Janus dumbbell” as illustrated in Fig. 1. This phase terminates in what we refer to as “the final fate” where no further gravitational waves are emitted. Naturally this phase either describes a nonrotating object or an axisymmetric, stationary, object. We recognize that during this post-merger phase there might be non-negligible energy loss via electromagnetic and scalar radiation or particle emission, (e.g. neutrinos in the case of neutron stars) which must also

be accounted for (for some recent examples see [19–24]). The change in energy of the binary system due to gravitational wave emission between these two stages is given by the difference between the orbital energy at the beginning of the merged phase and the residual energy in the rotation of the final object as well as any non-gravitational-wave energy loss,  $E_{\text{other}}$ ,

$$\Delta E_{\text{pm}} = -\left( \frac{1}{2}\mathcal{I}\Omega_{\text{insp}}^2 \right)_{\Delta=R_1+R_2} + \frac{1}{2}\mathcal{I}_f\Omega_f^2 + E_{\text{other}}, \quad (3)$$

where the moment of inertia of the final merged object is  $\mathcal{I}_f$ .

Combining Eq. (1) and Eq. (3), the total energy emitted in gravitational radiation is given by the gravitational potential energy of the two masses in contact less the residual rotational energy of the final object,

$$\begin{aligned} E_{\text{GW,CO}} &= -(\Delta E_{\text{insp}} + \Delta E_{\text{pm}}) \\ &= \frac{GM_1M_2}{\Delta} - \frac{1}{2}\mathcal{I}_f\Omega_f^2 - E_{\text{other}}. \end{aligned} \quad (4)$$

Examining the relative contribution from the inspiral and post-merger phases, if little energy is radiated or tied up in the rotation of the final state object, then more gravitational radiation could be emitted during the post-merger phase than during inspiral. For example, in the case of identical objects ( $M_1 = M_2 = M$ ,  $R_1 = R_2 = R$ ,  $C_1 = C_2 = C$ ,  $\tilde{\mathcal{I}}_1 = \tilde{\mathcal{I}}_2 = \tilde{\mathcal{I}}$ ) and  $\Omega_f \rightarrow 0$  (i.e. a phase ending in a nonrotating object), we have

$$\max[E_{\text{GW,CO}}] = \underbrace{\frac{(1-\tilde{\mathcal{I}})MC}{4}}_{\Delta E_{\text{insp}}} + \underbrace{\frac{(1+\tilde{\mathcal{I}})MC}{4}}_{\Delta E_{\text{merg}}} = \frac{MC}{2}. \quad (5)$$

Note that for constant density spheres ( $\tilde{\mathcal{I}} = 2/5$ ), 70% of the total energy in gravitational radiation can be emitted during the post-merger phase. This stage in the evolution can therefore be very significant in assessing the detectability of compact object mergers, as we discuss in more detail below.

How close a realistic scenario gets to the upper bound in Eq. (5) depends on the details of the merger scenario, the composition of the merging objects and the possible final fate of the merger. These will determine the amount of energy radiated and stored in the spin and mass of the final object. For ECOs, our knowledge is naturally restricted to a few proposed models and further limited by the small number of works that have explored the nonlinear regime described by the merger; indeed, to our knowledge, only boson stars have been studied in this context [12,25].

The case of neutron star mergers is on better footing, with significant efforts exploring their complex phenomenology during and after coalescence and including several

mechanisms through which the system can lose energy and redistribute angular momentum. A detailed estimate of the post-merger object's behavior must account for magnetohydrodynamical effects, as well as the possibility of mass shedding, emission in electromagnetic radiation and neutrinos in  $E_{\text{other}}$ . All of these potentially affect the lifetime of configurations with a time-dependent quadrupole. As a bound on the total energy emitted electromagnetically, we can appeal to the estimated energy emitted in short gamma ray bursts. Such bursts are thought to be driven by neutron star mergers, and the total energy emitted is of order  $E_{\text{GRB}} \sim 10^{51} \text{ ergs} \sim 10^{-3} M_{\odot}$ , far below the energy emitted in gravitational radiation. An even larger amount of energy is carried away by neutrinos, but this is still arguably smaller than that in gravitational waves [19,26]. Simulations of binary neutron star mergers also indicate that tidal effects arise during the inspiral phase [9,19,22–24,27,28], but they are small, especially for higher compaction cases (which, as we shall discuss, are the cases which could radiate more energy than the analog black hole system). These estimates imply that  $E_{\text{other}}$  will be small compared to the energy emitted in gravitational radiation. Finally, for neutron stars with the right masses and EoS, the time scale for the post-merger phase can be as long as  $10\text{--}10^4 \text{ s}$  [29,30]. Provided a time-varying quadrupole lasts this long, the system can potentially execute millions of post-merger orbital periods (see Sec. III), and allow a significant amount of energy to be emitted as gravitational radiation during the post-merger phase.

Assuming that  $E_{\text{other}}$  is negligible, the expression Eq. (5) provides a bound that depends on the compaction of the merging objects and the rotational energy of the final object. Assuming most of the gravitational binding energy is released as gravitational radiation and does not get locked in the rotational energy of the final object we can estimate an upper bound on the energy that could be emitted in a nonvacuum compact binary merger. In general, the total energy emitted increases with compaction. An upper bound on the compaction of spherically symmetric objects is given by Buchdal's theorem to be  $C \leq 4/9$  [31], which sets the maximum possible energy emitted in gravitational radiation during our envisioned merger. The emitted energy is greatest when the compaction of both objects is saturated at  $C_1 = C_2 = 4/9$ , yielding the bound,

$$E_{\text{GW,CO}} \leq \frac{4\mu}{9}. \quad (6)$$

For equal mass, nonspinning objects, this bound implies that the total energy emitted in gravitational radiation can reach up to  $\sim 11\%$  of the total rest mass of the system. Compare this value to that of the expected  $\sim 4\text{--}5\%$  of the total mass for equal mass, nonspinning binary black hole systems (e.g. [1,17,32]).

A lower limit on gravitational radiation in the post-merger phase can be computed by assuming that the final state, different from a black hole, is “instantaneously” produced conserving angular momentum. This fixes  $\Omega_f$  to be,

$$\Omega_f \simeq \frac{(\mathcal{I}\Omega_{\text{insp}})_{\Delta=R_1+R_2}}{\mathcal{I}_f}, \quad (7)$$

which implies that the energy change during the merger is

$$\Delta E_{\text{pm}} = -\left(1 - \frac{\mathcal{I}}{\mathcal{I}_f}\right) \left(\frac{1}{2} \mathcal{I} \Omega_{\text{insp}}^2\right)_{\Delta=R_1+R_2} + E_{\text{other}}. \quad (8)$$

$\Delta E_{\text{pm}}$  can be zero in this scenario. However, unless the initial ( $\mathcal{I}$ ) and final ( $\mathcal{I}_f$ ) moments of inertia are the same, energy must be dissipated in the form of gravitational radiation, electromagnetic radiation, neutrinos, mass shedding, etc. If  $\mathcal{I}$  is significantly different than  $\mathcal{I}_f$ , the energy loss can be an appreciable fraction of the total rest mass of the system. This is a simple motivation for the importance of searching for electromagnetic and neutrino counterparts to compact object mergers (e.g. [33–35]), which could elucidate the energy and momentum balance more effectively than observing a single channel.

In the absence of other radiation,  $E_{\text{other}}$ , and assuming no mass shedding, conservation of energy implies in this prompt-final-state scenario that  $\mathcal{I} \leq \mathcal{I}_f$ , which imposes a restriction on the configuration of the final fate object that can be produced in the merger. Imposing this requirement and assuming both the initial and final state objects are spherically symmetric with constant density, with the final object characterized by a compaction  $C_f$ , we bound  $C/C_f \geq \sqrt{7/8}$ , or equivalently,  $R_f/R \geq \sqrt{7/2}$ . The lower

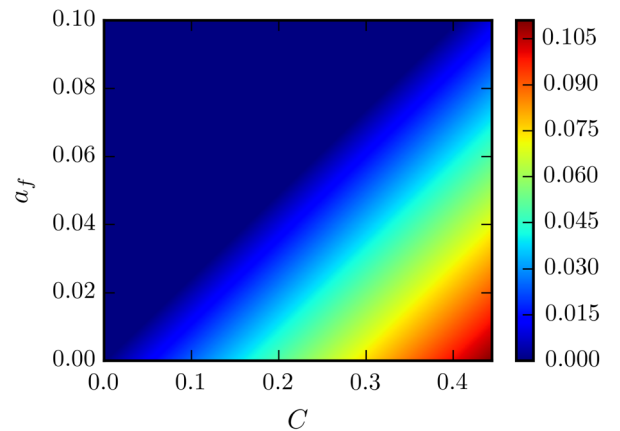


FIG. 2. The energy radiated per unit mass versus dimensionless final spin and final compaction for equal object binaries described by Eq. (4) and assuming equal mass, equal radius, and equal compaction objects merge to form a final object of maximal compaction ( $4/9$ ) and uniform density ( $\mathcal{I}_f = 2/5$ ).



bound for the emitted energy from the system is provided in this case by the inspiral phase, which we estimated in Eq. (5).

Between these upper and lower limits, there will be a range of merger scenarios in which the energy emitted in gravitational waves is larger than the corresponding black hole system. In Fig. 2 we show the energy radiated per unit mass versus dimensionless final spin and final compaction for equal object binaries described by Eq. (4). Assuming equal mass, equal radius, and equal compaction objects merge to form a final object of maximal compaction (4/9) and uniform density, the energy radiated can exceed that of the equivalent binary black hole system ( $\sim 4\%$ ) for a family of final objects with dimensionless spin  $a_f \equiv \Omega_f^2/M^2 \lesssim 0.07$  and  $C_f \gtrsim 0.15$ .

### B. A more realistic scenario: neutron star mergers

Numerical simulations of neutron star mergers provide a less idealized scenario than the one described above. Such simulations are already furnishing a more complete understanding of binary neutron star systems. However, such studies are computationally demanding due to the intrinsic cost associated with each one, the larger parameter space describing the binary (when compared to binary black holes systems), and the inclusion of different physical effects that can play a role over a disparate set of time and length scales. Here we employ some partial information inferred from simulations to enrich our model at a modest level while maintaining its simplicity. We begin by considering the post-merger neutron star is characterized, to leading order, by its rotation frequency and moment of inertia. Assuming conservation of angular momentum during the collision,

$$\mathcal{I}_f = \mathcal{I} \frac{\Omega_{\text{insp}}}{\Omega_{\text{pm}}}, \quad (9)$$

where  $\mathcal{I}$  and  $\Omega_{\text{insp}}$  are evaluated at  $\Delta = R_1 + R_2$ . During the post-merger phase, the change in energy due to emitted gravitational radiation is

$$\Delta E_{\text{pm}} = -\frac{1}{2} \mathcal{I}_f \Omega_{\text{pm}}^2 \quad (10)$$

$$= -\left(\frac{1}{2} \mathcal{I} \Omega_{\text{insp}}^2\right) \frac{\Omega_{\text{pm}}}{\Omega_{\text{insp}}}, \quad (11)$$

where we have omitted the terms in Eq. (11) associated with other forms of radiation and we assume that the final fate object does not rotate.

An estimate of the ratio of angular frequencies can be obtained in numerical relativity simulations, which indicate that  $\Omega_{\text{pm}}/\Omega_{\text{insp}} \approx 2$  (e.g. [19,20,36–38]) is a reasonable expectation, yielding,

$$\Delta E_{\text{pm}} = -\mathcal{I} \Omega_{\text{insp}}^2, \quad (12)$$

and therefore

$$E_{\text{GW,NS}} = \frac{1}{2} \mathcal{I} \Omega_{\text{insp}} + \frac{GM_1 M_2}{\Delta}. \quad (13)$$

Note that this is larger than the binding energy of the individual objects, and therefore in principle larger than in the toy model presented above. This is because: (i) we have neglected additional radiative degrees of freedom (which need not be significant depending on the objects involved) and (ii) some of the internal binding energy of the two objects has been converted to gravitational radiation in deforming the merging compact objects into the final compact object, which is reflected in the change in the moment of inertia.

In the case of the merger between identical objects and assuming the absence of other radiative degrees of freedom, we can again compare the total energy emitted by a binary neutron star system to an equivalent mass binary black hole system. The total energy emitted in the neutron star system is  $E_{\text{GW,NS}} = 17MC/20$ . Comparing against the energy emitted in the equivalent black hole system, the neutron star system will emit more total gravitational radiation as long as  $C > .14$ . This is comparable to reasonable compactness in neutron stars, implying that in principle a neutron star binary can emit more total gravitational radiation than the equivalent black hole system if there is no significant dissipation in other forms of energy and the final object is nonrotating; i.e. for relatively low total mass binaries that avoid collapse to a black hole (e.g. [39,40]).

### III. THE WAVEFORMS

The two polarizations of gravitational wave in our model are given by

$$\begin{aligned} h_+ &= \frac{4G\Omega^2\mu^2\Delta^2}{r} \cos(2\Omega t) \\ h_\times &= \frac{4G\Omega^2\mu^2\Delta^2}{r} \sin(2\Omega t). \end{aligned} \quad (14)$$

During the inspiral phase, both  $\Delta$  and  $\Omega$  evolve in time as the orbit decays. During the merger phase,  $\Delta = R_1 + R_2$  and only the frequency changes in time. The inspiral is associated with a chirp, e.g. an increase in frequency [41], but the merger is associated with an antichirp, which is a decrease in frequency as the merged, nonaxis-symmetric object spins down [42,43].

We can determine the time dependence of the frequency by computing the power emitted in gravitational waves and comparing to the time derivative of the orbital energy. The power emitted in gravitational waves is

$$\frac{dE}{dt} = -\frac{G}{5} \left\langle \frac{d^3 \mathbf{J}}{dt^3} \cdot \frac{d^3 \mathbf{J}}{dt^3} \right\rangle t, \quad (15)$$

where  $J_{ij}$  is the reduced quadrupole tensor. Assuming rotation along the  $z$ -axis of Cartesian coordinates, this is given by

$$\mathbf{J} = \frac{\mu \Delta^2}{2} \begin{pmatrix} \cos(2\Omega t) - \frac{1}{3} & \sin(2\Omega t) & 0 \\ \sin(2\Omega t) & -\cos(2\Omega t) - \frac{1}{3} & 0 \\ 0 & 0 & -\frac{2}{3} \end{pmatrix}, \quad (16)$$

which yields

$$\frac{dE}{dt} = -\frac{32G\mu^2\Delta^4\Omega^6}{5}. \quad (17)$$

During the inspiral phase, we can compare the power emitted in gravitational waves Eq. (17) to the time derivative of the orbital energy

$$\frac{dE}{dt} = \left[ \frac{GM_1 M_2}{\Delta^2} \frac{d\Delta}{d\Omega} + \mathcal{I}\Omega \right] \frac{d\Omega}{dt}, \quad (18)$$

in order to obtain the time derivative of the orbital frequency. During the early stages of inspiral where  $\Delta \gg R_1, R_2$ , we obtain

$$\frac{d\Omega}{dt} = 96G^{5/3}\mu M_{\text{tot}}^{2/3}\Omega^{11/3}. \quad (19)$$

During the merger phase,  $d\Delta/dt = 0$  in our simple model, and we therefore have

$$\frac{d\Omega}{dt} = -\frac{32G\mu^2\Delta^4\Omega^5}{5\mathcal{I}_{\Delta=R_1+R_2}}. \quad (20)$$

Setting the time of contact between the two compact objects to be  $t = 0$ , the solutions to Eq. (19) and (20) are

$$\Omega(t) = \frac{\Omega_{\text{insp}}}{(1 - \alpha_{\text{insp}} t)^{3/8}}, \quad t < 0 \quad (21)$$

$$\Omega(t) = \frac{\Omega_{\text{insp}}}{(1 + \alpha_{\text{pm}} t)^{1/4}}, \quad t > 0, \quad (22)$$

where the time constants  $\alpha_{\text{insp}}$  and  $\alpha_{\text{pm}}$  are given by

$$\alpha_{\text{insp}} = \frac{8\Omega_{\text{insp}}^{8/3}}{3} 96G^{5/3}\mu M_{\text{tot}}^{2/3} = \frac{32C^4}{GM}, \quad (23)$$

and

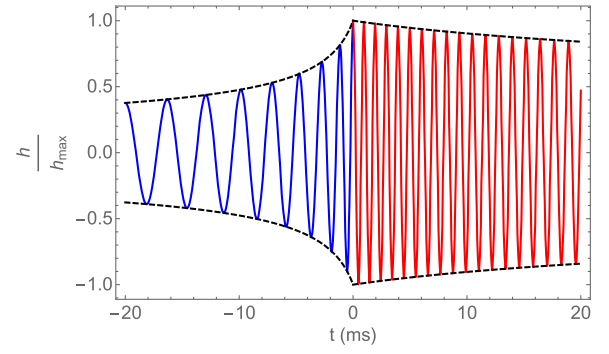


FIG. 3. An example of the waveform Eq. (14) for the merger of compact objects including an inspiral phase (blue) and ring down phase (red) for identical objects of mass  $M = M_\odot$  with  $C = .1$ . The chirp during inspiral has a higher pitch than the anti-chirp during ring down, creating a quasi-monochromatic signal during the post-merger phase.

$$\alpha_{\text{pm}} = 4\Omega_{\text{insp}}^4 \frac{32G\mu^2\Delta^4}{5\mathcal{I}_{\Delta=R_1+R_2}} = \frac{16C^4}{7GM}, \quad (24)$$

where  $\Omega_{\text{insp}} = \sqrt{GM_{\text{tot}}}(R_1 + R_2)^{-3/2} = C^{3/2}/(2GM)$  and in the second equality here and above we present the result for identical merging objects.

In Fig. 3 we sketch an example of the wave form for identical objects with  $C = .1$ , including both the inspiral and post-merger phases. The time constants set the characteristic rate of change of the frequency, while  $\Omega_{\text{insp}}$  sets the characteristic frequency. For identical objects of mass  $M = M_\odot$  and compactions of order  $C = 0.1$ , the time constants are approximately  $\alpha_{\text{insp}}^{-1} \approx 1.6$  ms and  $\alpha_{\text{pm}}^{-1} \approx 20$  ms. This can be compared to the orbital period at contact,  $\Omega_{\text{insp}}^{-1} = 0.3$  ms, which is far smaller than the decay time. Comparing with lifetimes of as long as  $10\text{--}10^4$  s for the time dependent quadrupole of merged neutron stars [29,30], we also see that the frequency can decay appreciably in realistic systems, which implies that a significant amount of energy is radiated in gravitational waves. More generally, the number of cycles compared to the time constants scales like  $\alpha_{\text{wd,insp}}/\Omega_{\text{insp}} \sim C^{-5/2}$ , which can be quite large for small compaction. Therefore, during the post-merger phase, the comparatively large frequency and slow decay of the frequency give rise to a nearly monochromatic signal.

Of course, our simple model captures the post-merger waveforms of realistic systems such as neutron star mergers only at a qualitative level. Missing from the model are: modulations in the waveforms resulting tidal effects as well as from compression/decompression of the merged object (in the case of neutron stars, see e.g. [23,37,44,45]), the main frequency of the early post-merger stages differing from  $\Omega_{\text{insp}}$  by a factor of  $\approx 2$  (for neutron stars, see e.g. [23]), additional modes resulting from normal modes of the

star, new modes resulting from possible instabilities [21,46,47], as well as additional physical effects driven by angular momentum transport and cooling (in neutron stars see, e.g. [7,19,20,48]) or interactions of characteristics fields of exotic compact objects (for the case of boson stars see [12]). The relevance and importance of each of these effects depends upon the nature of the merging objects. It is possible to enrich the model in order to account for some of these features, as has been done for neutron star mergers in Ref. [44]. However, careful modelling of specific systems is beyond the scope of the present work, which is intended only to provide a general rule of thumb for generic compact object mergers (detached as much as possible from specific cases), and a benchmark for comparison with black hole mergers of equivalent mass.

#### IV. DETECTABILITY

We have shown above that it is in principle possible for more total energy in gravitational radiation to be emitted in the merger of compact objects than in the equivalent mass black hole system. However, because gravitational wave detectors are sensitive only over a range of frequencies, this extra energy may or may not be easily detectable. In this section, we address the detectability of the gravitational waves emitted by the model described above.

An estimate of the signal to noise ratio (SNR) can be obtained assuming an optimal filter is applied to hypothetical time stream data. The square of the SNR is given in frequency space by [49]

$$\langle \text{SNR}^2 \rangle = 4 \int_0^\infty \frac{|h_{\text{char}}(f)|^2}{S_n(f)} df, \quad (25)$$

where  $S_n(f)$  is the one-sided noise power spectral density. We consider two representative spectral densities. The first

is the projected sensitivity of advanced LIGO [50], shown as the black line in Fig. 4, which for convenience we take to be infinity outside the interval  $10 \text{ Hz} < f < 4 \times 10^3 \text{ Hz}$ . The second is a scale invariant noise, defined in the same frequency interval as the LIGO sensitivity curve, given by  $h_n(f) \approx 3.5 \times 10^{-23} f^{-1/2}$ .

The one-sided signal power spectrum is defined as

$$h_{\text{char}}(f)^2 \equiv \frac{5G(1+z)^2}{8\pi^2 D_L(z)^2} f^{-2} \left| \frac{dE}{df} \right|_{(1+z)f}, \quad (26)$$

where  $z$  is the redshift to the binary,  $D_L(z)$  is the luminosity distance, and  $dE/df$  is the energy loss as a function of frequency evaluated at the redshifted frequency.

For a compact object merger with our model, the energy will vary differently with frequency during the inspiral and post-merger phases, so we analyze these two cases separately. Beginning with the inspiral phase, and identifying  $f = \Omega/\pi$ , we obtain

$$\left| \frac{dE}{df} \right|_{\text{insp}}(f < f_{\text{pm}}) = \frac{\pi^{2/3} G^{2/3}}{3} \mu M_{\text{tot}}^{2/3} f^{-1/3} - \pi^2 (\tilde{\mathcal{I}}_1 M_1 R_1^2 + \tilde{\mathcal{I}}_2 M_2 R_2^2) f, \quad (27)$$

where we have used the Keplerian relation between  $\Delta$  and  $\Omega$ , and  $f_{\text{pm}}$  is the frequency at the end of the inspiral phase, given by  $f_{\text{pm}} \equiv \sqrt{GM_{\text{tot}}/\pi^2 (R_1 + R_2)^{-3/2}}$ . Comparing this to the plunge frequency [51], for identical merging objects we have  $f_{\text{pm}} = f_{\text{pl}} C^{3/2} (\Delta_{\text{plunge}}/GM_{\text{tot}})^{3/2} \approx 6.55 C^{3/2} f_{\text{pl}}$ . Note that for compactions larger than  $C > .29$ , the merger frequency will be larger than the plunge frequency. During the post-merger phase, we obtain

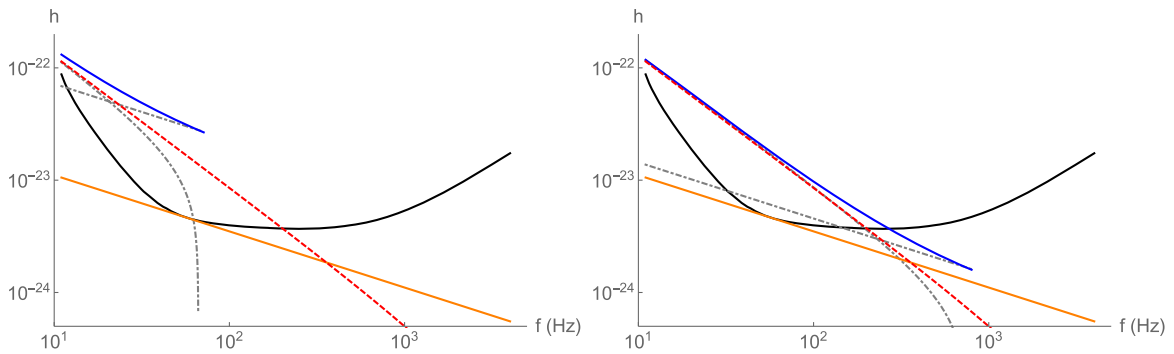


FIG. 4. Characteristic strain versus frequency for a variety of noise scenarios and merger events. The black solid line is the projected characteristic strain noise  $|h_n(f)|$  for advanced LIGO. The orange solid line is the characteristic strain noise in a scenario with scale-invariant sensitivity across the advanced LIGO frequency range. The red dashed line is the characteristic strain of a black hole-black hole merger with  $M_1 = M_2 = 1.25 M_\odot$  at a redshift of  $z = 0.01$ , computed in the PhenomD phenomenological model. The grey dot-dashed lines are the characteristic strain produced in the inspiral [Eq. (30)] and post-merger [Eq. (31)] phases of a compact object merger in our toy model with  $M_1 = M_2 = 1.25 M_\odot$  at a redshift of  $z = 0.01$  (the same as the fiducial black hole system) with  $\tilde{\mathcal{I}}_1 = \tilde{\mathcal{I}}_2 = 2/5$  and compaction  $C = 0.02$  (left panel) and  $C = 0.1$  (right panel). The total characteristic strain for the compact object merger (Eq. (29)) is shown as the solid blue line.

$$\left| \frac{dE}{df} \right|_{\text{pm}} (f_{\text{ff}} < f < f_{\text{pm}}) = \pi^2 \mathcal{I}_{\Delta=R_1+R_2} f \quad (28)$$

where  $f_{\text{ff}}$  is the frequency at which the post-merger phase terminates. Notice this frequency is  $< f_{\text{merg}}$  as a result of the spin-down of the post-merger object due to the emission of gravitational waves; in particular if the object retains its quadrupole, then  $f_{\text{ff}} = 0$ .

We consider the contributions to the characteristic strain from the inspiral and post-merger phases separately:

$$h_{\text{CO}}(f)^2 = h_{\text{CO,insp}}(f)^2 + h_{\text{CO,pm}}(f)^2 \quad (29)$$

where it is understood that  $h_{\text{CO,insp}}$  is defined in the interval  $f < f_{\text{merg}}$  and  $h_{\text{CO,merg}}$  is defined in the interval  $f_{\text{ff}} < f < f_{\text{merg}}$ . For the inspiral phase, we obtain:

$$\begin{aligned} h_{\text{CO,insp}}(f)^2 &\simeq \frac{5}{8} (1+z)^{5/3} \left( \frac{\text{Mpc}}{D_L(z)} \right)^2 \frac{\mu}{M_\odot} \left( \frac{M_{\text{tot}}}{M_\odot} \right)^{2/3} \\ &\times 10^{-38} \text{ Hz}^{1/3} f^{-7/3} \\ &- 0.78 (1+z)^3 \left[ \frac{\tilde{\mathcal{I}}_1}{C_1^2} \left( \frac{M_1}{M_\odot} \right)^3 + \frac{\tilde{\mathcal{I}}_2}{C_2^2} \left( \frac{M_2}{M_\odot} \right)^3 \right] \\ &\times \left( \frac{\text{Mpc}}{D_L(z)} \right)^2 f^{-1} \times 10^{-44} \text{ Hz}^{-1}. \end{aligned} \quad (30)$$

For the post-merger phase, we obtain:

$$\begin{aligned} h_{\text{CO,pm}}(f)^2 &\simeq 0.78 (1+z)^3 \times \left( \frac{\text{Mpc}}{D_L(z)} \right)^2 f^{-1} \times 10^{-44} \text{ Hz}^{-1} \\ &\times \left[ \frac{\tilde{\mathcal{I}}_1}{C_1^2} \left( \frac{M_1}{M_\odot} \right)^3 + \frac{\tilde{\mathcal{I}}_2}{C_2^2} \left( \frac{M_2}{M_\odot} \right)^3 \right. \\ &\left. + \frac{\mu}{M_\odot} \left( \frac{M_1}{M_\odot C_1} + \frac{M_2}{M_\odot C_2} \right)^2 \right]. \end{aligned} \quad (31)$$

We can now compare our compact binary model with a binary black hole waveform. To properly capture the merger and ring-down phases, we adopt the “PhenomD” model [52], one of the phenomenological waveform models that has been tuned with numerical relativity simulations.

In Fig. 4, we show the characteristic strain for a system of two compact objects of mass  $M_1 = M_2 = 1.25 M_\odot$  at a redshift of  $z = 0.01$  (the same as the fiducial black hole system) with  $\tilde{\mathcal{I}}_1 = \tilde{\mathcal{I}}_2 = 2/5$  and compaction  $C = 0.02$  (left panel) and  $C = 0.1$  (right panel). For these masses, a long-lived neutron star is a likely outcome of the merger. Here, we have assumed that  $f_{\text{ff}}$  lies outside the frequency range of the sensitivity curves. The dashed grey curves show the contribution from  $h_{\text{CO,pm}}^2$  and  $h_{\text{CO,insp}}^2$ , while the blue curve shows their sum. The relative SNR between the

compact object and black hole systems is both a function of the compaction and of the strain noise.

To examine the relative SNR quantitatively, in Fig. 5 we plot the SNR of the fiducial black hole system and an equivalent mass system of identical compact objects from our model, as a function of the compaction. The result for the advanced LIGO strain noise is shown in blue, with the corresponding SNR for the black hole shown as the dashed blue curve. The result for the scale invariant strain noise is shown in orange, with the corresponding SNR for the black hole shown as the dashed orange curve. We have again assumed that  $f_{\text{ff}}$  lies outside (and below) the frequency range of the sensitivity curves. The SNR is larger than the corresponding black hole system for compactations larger than  $C \sim .015$  for the advanced LIGO strain noise scenario and  $C \sim .01$  for the scale invariant noise scenario. The growth in the SNR with compaction for the scale invariant sensitivity curve is in accord with the intuition that systems where more total energy is emitted are also more detectable. For the LIGO sensitivity curve, the story is a little more complicated. Since LIGO is not sensitive to the majority of the gravitational radiation emitted in the post-merger phase for this fiducial example at large compaction, the SNR first rises then falls. However, for all but the largest compactations where the post-merger phase for the compact objects exits the LIGO sensitivity window, the cases where more total energy is emitted are also more detectable.

Scanning a range of masses [53] between  $M_\odot < M < 30 M_\odot$ , we found the compaction that yields the maximum boost in SNR over the equivalent mass black hole system for the advanced LIGO and scale invariant sensitivity strain noise scenarios. For the advanced LIGO case, the maximum boost in squared SNR is nearly flat over redshift and mass, equal to  $\sim 1.8$ – $2.5$ . The compaction at which the maximum boost occurs increases with mass and is relatively independent of redshift, ranging from  $C \sim .03$  for  $M = M_\odot$  to  $C \sim .25$  for  $M = 30 M_\odot$ . For the scale invariant sensitivity scenario, the maximum boost is

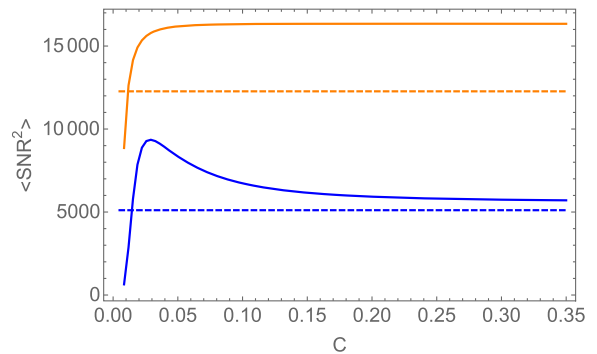


FIG. 5. The SNR squared (Eq. (25)) for the fiducial compact object mergers shown in Fig. 4 as a function of compaction for the advanced LIGO (blue) and scale invariant sensitivity (orange) strain noise scenarios. The SNR squared for the corresponding black hole systems are shown as dashed lines.



similar, relatively flat over the parameter space and of order  $\sim 1.3$ – $2.0$ . The compaction at which the maximum occurs, however, is always saturated at the maximum value (see Fig. 5), which in this case is  $C = 4/9$ .

We conclude that compact object mergers can, in principle, emit more total gravitational energy than their counterpart black hole system and can generally be more detectable with present detectors provided, of course, the conditions described are met. The boost in SNR is  $\sim \sqrt{2}$ .

## V. CONCLUSIONS

In this paper we have investigated a toy model binary merger of two compact objects that can in principle emit more energy in gravitational radiation than a black hole system of equivalent mass. While very simplistic, this model illustrates what might be possible in more realistic systems such as the merger of two neutron stars, or perhaps more exotic compact objects. We have found that the merger of objects with compactions of order  $C \sim \mathcal{O}(0.1)$  and larger that avoid collapse to a black hole can yield more energy in gravitational radiation than the corresponding black hole system by up to a factor of roughly two. The SNR for such compact object mergers in a gravitational wave detector such as advanced LIGO can exceed that of the corresponding black hole merger by a factor of  $\sim \sqrt{2}$  for somewhat smaller compactions  $C \sim \mathcal{O}(0.03)$ . This is in accord with the two-fold increase in total energy emitted in the most optimistic merger scenario.

Compact object mergers have the potential to radiate more energy and be more detectable than the merger of equivalent mass black holes, but do they? This depends somewhat on how representative the assumptions underlying our toy model are. First, we have assumed that the only sink for orbital energy is in the form of gravitational radiation. This is clearly incorrect, as in any realistic scenario energy will be dissipated mechanically in the deformation of the objects, radiatively through electromagnetic (and possibly scalar) radiation, or through neutrino (or other particles) emission. A complete treatment accounting for this would influence the total energy emitted, and the energy spectrum of the outgoing gravitational waves, which could change the prospects for detectability. We have also been generous in assuming that the post-merger

phase terminates at frequencies lower than 10 Hz (i.e. below the lowest in the LIGO band). Relaxing this assumption would diminish the boost in detectability. Additionally, we have neglected general relativistic and tidal effects on the inspiral and post-merger phases. For large compactions as those we have considered, these effects are arguably small [54,55]. Finally, we have also considered nonspinning objects. Black holes could in principle be highly spinning and, if relatively well aligned with the orbital angular momentum, their total radiated energy could be considerably higher [56]. On the other hand, as in the case of neutron stars, a bound on the spin of non-vacuum compact objects could exist to prevent mass shedding; consequently spin might only modestly boost the energy radiated in such cases. Nevertheless, according to current estimates of the projected spin along the orbital angular momentum through gravitational waves, this is low [58]; thus our no-spin treatment in this work does not appear to be overly restrictive.

These loose ends motivate a more systematic treatment which, in turn, involves specializing to specific objects (see e.g. [44,59]) with all the implications/physical requirements that their analysis would require.

Given the impending flood of data from LIGO and future gravitational wave detectors, we stand to learn a great deal about sources of gravitational radiation in our Universe. Since compact object mergers can in principle both yield more energy in gravitational radiation and be more detectable by advanced LIGO, it is important to keep an open mind about what surprises might await, and strive to gain some idea about how big such a surprise might be.

## ACKNOWLEDGMENTS

M. C. J. and L. L. are supported by the National Science and Engineering Research Council through a Discovery grant. L. L. also thanks CIFAR for support. C. H. thanks the NSF Grant No. PHY-1454389. This research was supported in part by Perimeter Institute for Theoretical Physics. Research at Perimeter Institute is supported by the Government of Canada through the Department of Innovation, Science and Economic Development Canada and by the Province of Ontario through the Ministry of Research, Innovation and Science.

- 
- [1] B. P. Abbott, R. Abbott, T. D. Abbott, M. R. Abernathy, F. Acernese, K. Ackley, C. Adams, T. Adams, P. Addesso, R. X. Adhikari *et al.* (LIGO Scientific Collaboration and Virgo Collaboration), *Phys. Rev. Lett.* **116**, 061102 (2016).
  - [2] B. P. Abbott *et al.* (Virgo, LIGO Scientific Collaborations), *Phys. Rev. Lett.* **116**, 241103 (2016).

- [3] B. Abbott *et al.* (LIGO Scientific Collaboration and Virgo Collaboration), *Astrophys. J. Lett.* **832**, L21 (2016).
- [4] As evidenced by the ability to simple, first principle models, to relatively accurately capture the final state of the system [5,6].
- [5] A. Buonanno, L. E. Kidder, and L. Lehner, *Phys. Rev. D* **77**, 026004 (2008).

- [6] M. Kesden, G. Lockhart, and E. S. Phinney, *Phys. Rev. D* **82**, 124045 (2010).
- [7] Y. Sekiguchi, K. Kiuchi, K. Kyutoku, and M. Shibata, *Prog. Theor. Exp. Phys.* **2012**, 01A304 (2012).
- [8] L. Lehner and F. Pretorius, *Annu. Rev. Astron. Astrophys.* **52**, 661 (2014).
- [9] L. Baiotti and L. Rezzolla, *arXiv:1607.03540*.
- [10] That is, when the total mass of the newly formed star is  $\gtrsim 1.2M_{\text{max}}$  where  $M_{\text{max}}$  is the maximum allowed mass for a stable star with the corresponding equation of state (rotation providing the additional support above this value).
- [11] K. Hotokezaka, K. Kyutoku, H. Okawa, M. Shibata, and K. Kiuchi, *Phys. Rev. D* **83**, 124008 (2011).
- [12] C. Palenzuela, L. Lehner, and S. L. Liebling, *Phys. Rev. D* **77**, 044036 (2008).
- [13] C. B. M. H. Chirenti and L. Rezzolla, *Classical Quantum Gravity* **24**, 4191 (2007).
- [14] J. D. Bekenstein, *Phys. Rev. D* **7**, 2333 (1973).
- [15] R. Penrose and R. Floyd, *Nature (London)* **229**, 177 (1971).
- [16] R. D. Blandford and R. L. Znajek, *Mon. Not. R. Astron. Soc.* **179**, 433 (1977).
- [17] D. Pollney, C. Reisswig, E. Schnetter, N. Dorband, and P. Diener, *Phys. Rev. D* **83**, 044045 (2011).
- [18] L. S. Grigorian and H. F. Khachatryan, *Astrophysics (Engl. Transl.)* **40**, 327 (1997).
- [19] C. Palenzuela, S. L. Liebling, D. Neilsen, L. Lehner, O. L. Caballero, E. O'Connor, and M. Anderson, *Phys. Rev. D* **92**, 044045 (2015).
- [20] F. Foucart, R. Haas, M. D. Duez, E. O'Connor, C. D. Ott, L. Roberts, L. E. Kidder, J. Lippuner, H. P. Pfeiffer, and M. A. Scheel, *Phys. Rev. D* **93**, 044019 (2016).
- [21] W. E. East, V. Paschalidis, F. Pretorius, and S. L. Shapiro, *Phys. Rev. D* **93**, 024011 (2016).
- [22] Y. Sekiguchi, K. Kiuchi, K. Kyutoku, M. Shibata, and K. Taniguchi, *Phys. Rev. D* **93**, 124046 (2016).
- [23] L. Lehner, S. L. Liebling, C. Palenzuela, O. L. Caballero, E. O'Connor, M. Anderson, and D. Neilsen, *Classical Quantum Gravity* **33**, 184002 (2016).
- [24] D. Radice, F. Galeazzi, J. Lippuner, L. F. Roberts, C. D. Ott, and L. Rezzolla, *Mon. Not. R. Astron. Soc.* **460**, 3255 (2016).
- [25] S. L. Liebling and C. Palenzuela, *Living Rev. Relativ.* **15**, 6 (2012).
- [26] Y. Sekiguchi, K. Kiuchi, K. Kyutoku, and M. Shibata, *Phys. Rev. Lett.* **107**, 051102 (2011).
- [27] S. Rosswog, M. Liebendoerfer, F. K. Thielemann, M. B. Davies, W. Benz, and T. Piran, *Astron. Astrophys.* **341**, 499 (1999).
- [28] D. Martin, A. Perego, A. Arcones, F.-K. Thielemann, O. Korobkin, and S. Rosswog, *Astrophys. J.* **813**, 2 (2015).
- [29] V. Ravi and P. D. Lasky, *Mon. Not. R. Astron. Soc.* **441**, 2433 (2014).
- [30] W. Kastaun, R. Ciolfi, and B. Giacomazzo, *Phys. Rev. D* **94**, 044060 (2016).
- [31] C. Misner, K. Thorne, and J. Wheeler, *Gravitation* (W.H. Freeman and Company, San Francisco, 1973).
- [32] M. Hannam *et al.*, *Phys. Rev. D* **79**, 084025 (2009).
- [33] J. S. Bloom *et al.*, *arXiv:0902.1527*.
- [34] B. D. Metzger and E. Berger, *Astrophys. J.* **746**, 48 (2012).
- [35] N. Andersson *et al.*, *Classical Quantum Gravity* **30**, 193002 (2013).
- [36] W. Kastaun and F. Galeazzi, *Phys. Rev. D* **91**, 064027 (2015).
- [37] A. Bauswein and N. Stergioulas, *Phys. Rev. D* **91**, 124056 (2015).
- [38] K. Hotokezaka, K. Kyutoku, Y.-i. Sekiguchi, and M. Shibata, *Phys. Rev. D* **93**, 064082 (2016).
- [39] A. Bauswein, T. W. Baumgarte, and H. T. Janka, *Phys. Rev. Lett.* **111**, 131101 (2013).
- [40] M. Shibata, *Numerical Relativity*, 100 Years of General Relativity (World Scientific Publishing Company, Singapore, 2015).
- [41] P. C. Peters and J. Mathews, *Phys. Rev.* **131**, 435 (1963).
- [42] H. Melosh, *Nature (London)* **224**, 781 (1969).
- [43] W. H. Press and K. S. Thorne, *Annu. Rev. Astron. Astrophys.* **10**, 335 (1972).
- [44] K. Takami, L. Rezzolla, and L. Baiotti, *Phys. Rev. D* **91**, 064001 (2015).
- [45] S. Bernuzzi, T. Dietrich, and A. Nagar, *Phys. Rev. Lett.* **115**, 091101 (2015).
- [46] D. Radice, S. Bernuzzi, and C. D. Ott, *Phys. Rev. D* **94**, 064011 (2016).
- [47] L. Lehner, S. L. Liebling, C. Palenzuela, and P. Motl, *Phys. Rev. D* **94**, 043003 (2016).
- [48] M. Anderson, E. W. Hirschmann, L. Lehner, S. L. Liebling, P. M. Motl, D. Neilsen, C. Palenzuela, and J. E. Tohline, *Phys. Rev. Lett.* **100**, 191101 (2008).
- [49] B. Allen, W. G. Anderson, P. R. Brady, D. A. Brown, and J. D. Creighton, *Phys. Rev. D* **85**, 122006 (2012).
- [50] J. Aasi *et al.* (VIRGO, LIGO Scientific Collaborations), *Living Rev. Relativ.* **19**, 1 (2016).
- [51] The transition from inspiral to the merger phase happens at the orbital radius past which there are no stable circular orbits, corresponding to the plunge frequency in the wave form. To a rather good approximation the plunge frequency,  $\Delta_{\text{plunge}}$ , can be obtained via first-principles as described in [5,6]. For nearly equal mass non-spinning black holes  $\Delta_{\text{plunge}} \approx 3.5GM_{\text{tot}}$ , yielding  $f_{\text{pl}} \approx 0.048(GM_{\text{tot}})^{-1}$ .
- [52] S. Khan, S. Husa, M. Hannam, F. Ohme, M. Pürrer, X. J. Forteza, and A. Bohé, *Phys. Rev. D* **93**, 044007 (2016).
- [53] Naturally, this range of masses is too large for NSs which would be bounded by  $< 3 M_{\odot}$ . However, mass bounds for exotic compact objects are, so far, largely unconstrained.
- [54] T. Mora and C. M. Will, *Phys. Rev. D* **69**, 104021 (2004); **71**, 129901(E) (2005).
- [55] E. Poisson and C. M. Will, *Gravity: Newtonian, Post-Newtonian, Relativistic* (Cambridge University Press, Cambridge UK, 2014).
- [56] Which could be as high as 12.5% of the total mass of the system for low eccentricity mergers. This estimate, obtained through [5], does not take into account the amount of energy radiated from the ISCO onwards, but this is small for this extreme scenario. Indeed, the estimate is in excellent agreement with numerical results of highly spinning binary black hole mergers [57].
- [57] M. A. Scheel, M. Giesler, D. A. Hemberger, G. Lovelace, K. Kuper, M. Boyle, B. Szilágyi, and L. E. Kidder, *Classical Quantum Gravity* **32**, 105009 (2015).
- [58] B. P. Abbott *et al.* (Virgo, LIGO Scientific Collaborations), *Phys. Rev. X* **6**, 041015 (2016).
- [59] T. Hinderer *et al.*, *Phys. Rev. Lett.* **116**, 181101 (2016).